THE JOURNAL OF BIOLOGICAL CHEMISTRY VOL. 291, NO. 15, pp. 8004–8013, April 8, 2016

Kinetics of Nitrite Reduction and Peroxynitrite Formation by Ferrous Heme in Human Cystathionine β-Synthase*

Received for publication, January 29, 2016 Published, JBC Papers in Press, February 11, 2016, DOI 10.1074/jbc.M116.718734

Sebastián Carballal[‡§1], Ernesto Cuevasanta[§¶], Pramod K. Yadav[‖], Carmen Gherasim[‖], David P. Ballou[‖], Beatriz Alvarez[§¶], and Ruma Banerjee[‖2]

From the [‡]Departamento de Bioquímica, Facultad de Medicina, [§]Center for Free Radical and Biomedical Research, and [¶]Laboratorio de Enzimología, Facultad de Ciencias, Universidad de la República, Montevideo 11800, Uruguay and the [‖]Department of Biological Chemistry, Medical Center, University of Michigan, Ann Arbor, Michigan 48109-0600

Cystathionine β-synthase (CBS) is a pyridoxal phosphate-dependent enzyme that catalyzes the condensation of homocysteine with serine or with cysteine to form cystathionine and either water or hydrogen sulfide, respectively. Human CBS possesses a noncatalytic heme cofactor with cysteine and histidine as ligands, which in its oxidized state is relatively unreactive. Ferric CBS (Fe(III)-CBS) can be reduced by strong chemical and biochemical reductants to Fe(II)-CBS, which can bind carbon monoxide (CO) or nitric oxide ($NO^{\bullet}$), leading to inactive enzyme. Alternatively, Fe(II)-CBS can be reoxidized by O_2 to Fe(III)-CBS, forming superoxide radical anion ($O_2^{\bullet-}$). In this study, we describe the kinetics of nitrite (NO_2^-) reduction by Fe(II)-CBS to form Fe(II)$NO^{\bullet}$-CBS. The second order rate constant for the reaction of Fe(II)-CBS with nitrite was obtained at low dithionite concentrations. Reoxidation of Fe(II)$NO^{\bullet}$-CBS by O_2 showed complex kinetic behavior and led to peroxynitrite ($ONOO^-$) formation, which was detected using the fluorescent probe, coumarin boronic acid. Thus, in addition to being a potential source of superoxide radical, CBS constitutes a previously unrecognized source of $NO^{\bullet}$ and peroxynitrite.

Cystathionine β-synthase (CBS)[3] is a key enzyme in the metabolism of sulfur amino acids in mammals. It catalyzes the pyridoxal 5′-phosphate (PLP)-dependent condensation of serine with homocysteine to give cystathionine and water in the first step of the trans-sulfuration pathway that leads to cysteine. CBS also condenses homocysteine and cysteine to form cystathionine and H_2S, a newly recognized physiological modulator with a broad range of effects in the cardiovascular, gastrointestinal, and nervous systems (1–3). An increased level of homocysteine in plasma constitutes a risk factor for cardiovascular diseases and is correlated with neural tube defects and Alzheimer's disease (4–7). Inborn errors of metabolism caused by mutations in CBS represent the most common cause of inherited hyperhomocysteinemia (8). Full-length human CBS has a subunit molecular mass of ~63 kDa and exists as a homodimer or as higher order oligomers (9). Each monomer has a modular organization that comprises an N-terminal domain that binds heme, followed by a catalytic domain that binds PLP, and a C-terminal regulatory domain that binds the allosteric activator, *S*-adenosyl-L-methionine (AdoMet). CBS activity increases in the presence of AdoMet or by limited proteolysis that results in the separation of the regulatory domain and formation of a truncated catalytic core (10–13).

The b-type heme in human CBS has a low spin and six-coordinate iron in both the ferric and ferrous states (14), with Cys^{52} and His^{65} serving as the axial ligands (10, 12, 15, 16). The heme environment is conserved in CBS among several eukaryotic species but does not resemble any other known heme protein (17, 18). Although a direct role for the heme in the PLP-dependent enzymatic mechanism was excluded (19), a regulatory role has been proposed on the basis of the observation that perturbations in the heme coordination environment can modulate enzyme activity through shifts in the PLP tautomeric equilibrium. Communication between the heme and PLP sites is transmitted via an α-helix that interacts at one end with the Cys^{52} heme ligand via Arg^{266} and at the other end with PLP via two conserved threonine residues (Thr^{257} and Thr^{260}) (18, 20–24).

Ferric CBS is quite stable and inert to exogenous ligands (16, 25). It is sensitive, however, to the thiophilic cation mercury(II) and to the strong oxidant and nitrating agent peroxynitrite ($ONOO^-$)[4] (26, 27). Despite the fairly low heme reduction potential of −0.350 V (21), CBS reduction can potentially be accomplished *in vivo* by enzymatic oxidoreductases. We have

* This work was supported by grants and fellowships from Universidad de la República (Comisión Sectorial de Investigación Científica (CSIC) (to B. A. and E. C.) and Comisión Académica de Posgrado (CAP) (to E. C.)), L'Oréal-Unesco, Uruguay (to B. A.), a PROLAB Grant from the American Society for Biochemistry and Molecular Biology (to S. C.), National Institutes of Health Grant HL58984 (to R. B.), and American Heart Association Postdoctoral Fellowship 14POST18760003 (to P. K. Y). The authors declare that they have no conflicts of interest with the contents of this article. The content is solely the responsibility of the authors and does not necessarily represent the official views of the National Institutes of Health.

[1] To whom correspondence may be addressed: Departamento de Bioquímica, Facultad de Medicina, Universidad de la República, Avda. Gral. Flores 2125, 11800 Montevideo, Uruguay. Tel.: 598-29249561; E-mail: scarballal@fmed.edu.uy or scarballal@gmail.com.

[2] To whom correspondence may be addressed: 4220C MSRB III, 1150 W. Medical Center Dr., University of Michigan, Ann Arbor, MI 48109-0600. Tel.: 734-615-5238; E-mail: rbanerje@umich.edu.

[3] The abbreviations used are: CBS, cystathionine β-synthase; Fe(III)-CBS, CBS with ferric heme; Fe(II)-CBS, CBS with ferrous heme; Fe(II)$NO^{\bullet}$-CBS, CBS with ferrous heme ligated to $NO^{\bullet}$; Fe(II)CO-CBS, CBS with ferrous heme ligated to CO; Fe(II)424-CBS, CBS with ferrous heme and a neutral ligand replacing cysteine; PLP, pyridoxal 5′-phosphate; AdoMet, *S*-adenosyl-L-methionine; DTPA, diethylenetriaminepentaacetic acid; CBA, coumarin-7-boronic acid; COH, 7-hydroxycoumarin.

[4] The term peroxynitrite ($ONOO^-$) is used to refer to the species in equilibrium, peroxynitrite anion ($ONOO^-$) and peroxynitrous acid (ONOOH). IUPAC recommended names are oxoperoxonitrate (1−) and hydrogen oxoperoxonitrate, respectively.

previously demonstrated that the cytosolic diflavin-containing methionine synthase reductase, in the presence of NADPH as electron donor, is able to reduce the heme in CBS (28, 29). In the reduced form, Fe(II)-CBS can react with O_2, and it can also bind CO and NO•. The reaction of Fe(II)-CBS with O_2 occurs rapidly with a second order rate constant of $(1.13 \pm 0.05) \times 10^5$ M^{-1} s^{-1} (pH 7.4, 25 °C), leading to the formation of Fe(III)-CBS and superoxide radical anion ($O_2^{\cdot-}$) (30). Fe(II)-CBS can bind CO, which replaces the axial cysteine ligand, forming Fe(II)CO-CBS. The observed rate constants increase hyperbolically with CO concentration, reaching limiting values of 0.012–0.017 s^{-1} at 25 °C (31, 32) or 0.0031 s^{-1} at 1 mM CO (28). Relevantly, Fe(II)CO-CBS displays decreased catalytic activity, with a K_i for CO of ~5.6 μM, which might be within a physiologically relevant concentration range (31, 33). Exposure of Fe(II)CO-CBS to O_2 results in its rapid reoxidation to Fe(III)-CBS concomitant with recovery of enzyme activity (29). In contrast to CO, NO• binding to Fe(II)-CBS results in a pentacoordinate iron-nitrosyl Fe(II)NO•-CBS species with a Soret maximum at 394 nm, indicating the loss of both endogenous axial ligands (34). It was recently reported that NO• binds with a $K_d \leq 0.23$ μM and with kinetic rate constants k_{on} of $\sim 8 \times 10^3$ M^{-1} s^{-1} and k_{off} of 0.003 s^{-1} (32). In addition, Fe(II)-CBS can slowly decay to an inactive Fe(II)424-CBS form with a Soret maximum at 424 nm, in which the cysteine is replaced by an unidentified neutral ligand (35, 36). Although Fe(II)424-CBS formation is promoted under nonphysiological conditions such as high temperature (36), the biological significance of this process is not clear. We have demonstrated recently that Fe(II)-CBS has the ability to reduce nitrite (NO_2^-) to NO•, leading to Fe(II)NO•-CBS formation, suggesting a possible new role for CBS in NO• signaling (37).

In this study, we have characterized the kinetics of nitrite reduction by the ferrous form of human CBS using low dithionite concentrations. We have also investigated the kinetics of Fe(II)NO•-CBS reoxidation by O_2 and examined the formation of peroxynitrite in the process. Overall, our results provide new insights into the kinetics of heme-mediated regulation of human CBS.

Experimental Procedures

Materials—All reagents were purchased from Sigma unless otherwise specified. Coumarin boronic acid (CBA) and peroxynitrite were from Cayman Chemical (Ann Arbor, MI). CBA was first dissolved in DMSO and then added directly to the samples to obtain the desired final concentration. The concentration of peroxynitrite was determined at 302 nm ($\epsilon = 1{,}670$ M^{-1} cm^{-1} (38)), and the stock solution was diluted in 10 mM NaOH immediately before use. Recombinant full-length wild-type and T257I human CBS and the truncated ΔC143-CBS variant were purified as described previously (24, 39). Protein concentration was determined by the Bradford method using bovine serum albumin as standard (40) and by using the reported extinction coefficients for CBS protein and heme (30). Reduction of Fe(III)-CBS was performed under a nitrogen atmosphere by the addition of known aliquots of sodium dithionite ($Na_2S_2O_4$) and confirmed by the appearance of the 449-nm Soret peak in the UV-visible absorption spectrum. Dithionite stock solutions were prepared in nitrogen-degassed 0.1 M NaOH and quantified by ferricyanide reduction ($\epsilon_{420} = 1{,}020$ M^{-1} cm^{-1}) (41) assuming a 2:1 (ferricyanide:dithionite) stoichiometry, in agreement with the actual reductant being the dithionite dissociation product $SO_2^{\cdot-}$. Solutions of sodium nitrite were prepared under anaerobic conditions and kept under a positive pressure of argon.

Kinetics of Fe(II)-CBS Reaction with Nitrite—An anaerobic solution of Fe(III)-CBS (1–10 μM) in phosphate buffer (0.1 M, pH 7.4, 0.1 mM diethylenetriaminepentaacetic acid (DTPA)) was reduced with low dithionite concentrations (10–15 μM) in an anaerobic chamber (Vacuum Atmospheres Co., Hawthorne, CA; 95/5 N_2/H_2 and <0.3 ppm O_2). The resulting Fe(II)-CBS solution was then mixed with a series of sodium nitrite concentrations at 37 °C, and the UV-visible absorption spectra were recorded outside the anaerobic chamber. Alternatively, stopped flow mixing was performed using a stopped flow spectrophotometer (SX.MV18; Applied Photophysics) equipped with a diode array detector, placed inside an anaerobic chamber. To avoid photochemical artifacts, the amount of incident white light was limited by adjusting the slit to 1 mm.

Kinetics of Fe(II)NO•-CBS Reoxidation by O_2—Fe(II)NO•-CBS solutions were prepared inside the anaerobic chamber. An anaerobic solution of Fe(III)-CBS (10 μM) in phosphate buffer (0.1 M, pH 7.4, with 0.1 mM (DTPA) was reduced with dithionite (90 μM), and heme reduction was monitored spectrophotometrically by a shift in the Soret peak from 428 to 449 nm. Sodium nitrite was added, and Fe(II)NO•-CBS formation was confirmed by a shift of the Soret peak to 394 nm. Excess dithionite and nitrite were removed by gel filtration using Micro Bio-Spin columns (Bio-Rad). The reaction mixtures containing the anaerobic solution of Fe(II)NO•-CBS were placed in cuvettes, sealed with a rubber septum, and purged with certified 100% O_2 (final concentration, ~1.25 mM), air (21% O_2), or mixed with solutions of increasing O_2 concentrations obtained by mixing different volumes of anaerobic and O_2-equilibrated water. The experiments were performed at 25.0 ± 0.1 °C.

Peroxynitrite Formation by Fe(II)NO•-CBS Exposed to O_2—The generation of peroxynitrite was determined using the boronate-based probe, CBA, and monitored by the increase in fluorescence intensity (excitation at 330 nm, emission at 450 nm) because of formation of the corresponding hydroxylated compound, 7-hydroxycoumarin (COH) (42). The procedure was calibrated using authentic peroxynitrite, and fluorescence spectroscopy was similar to that previously reported (42), with the intensity of the excitation and emission bands increasing linearly with peroxynitrite concentrations (data not shown). Typical reaction mixtures were prepared in the anaerobic chamber and contained Fe(III)-CBS (15 μM) in phosphate buffer (0.1 M, pH 7.4, with 0.1 mM DTPA) to which dithionite (100 μM) was added. After heme reduction, sodium nitrite (4 mM) was added, and Fe(II)NO•-CBS formation was confirmed spectrophotometrically, followed by gel filtration to avoid possible interference from nitrite or dithionite. Then Fe(II)NO•-CBS was placed in a fluorescence cuvette, and CBA was added. The cuvette was sealed with a rubber septum, and outside the anaerobic chamber, water-equilibrated with O_2 (100%) was added. Final concentrations were ~ 7.5, 20, and 625 μM for

Fe(II)NO•-CBS, CBA, and O_2, respectively. Florescence was registered at 25 °C in a Shimadzu 5031 PC spectrofluorimeter. To minimize photochemical artifacts, the incident light was diminished by decreasing the slit width to 1.5 mm and by recording the fluorescence every 10 min. At the end of the experiment, the cuvette was placed in the spectrophotometer to record the UV-visible spectrum of the heme. Controls showed that Fe(II)NO•-CBS and Fe(III)-CBS did not interfere with COH fluorescence intensity; neither did dithionite (below 600 μM). In some experiments, cysteine (5 mM), glutathione (20 mM), superoxide dismutase (875 units/ml, ~ 5.5 μM), or catalase (0.1 μM) was added.

Simulations and Data Analysis—Kinetic traces were analyzed and fitted using OriginPro 8. Data from the stopped flow experiments were fitted using the Pro-Data Viewer Software (Applied Photophysics). Computer-assisted kinetic simulations were performed with Gepasi (43). All experiments were repeated at least three times, and representative data are shown.

Results

Kinetics of Fe(II)-CBS Reaction with Nitrite—When an anaerobic solution of CBS was reduced with dithionite and mixed with nitrite, the characteristic Soret maximum of Fe(II)-CBS at 449 nm was converted to the five-coordinate Fe(II)NO•-CBS species, confirmed by the appearance of a 394 nm peak as reported previously (32, 34, 37) (Fig. 1*A*). This is consistent with the reaction of Fe(II)-CBS with nitrite to form Fe(III)-CBS and NO•. In the presence of reducing equivalents, this is followed by the reaction of Fe(II)-CBS with NO• to yield Fe(II)NO•-CBS (reactions 1–3), in analogy to the mechanism proposed for globins (44–47).

$$\text{Fe(II)-CBS} + NO_2^- + H^+ \rightarrow \text{Fe(III)-CBS} + NO^\bullet + OH^- \quad \text{(Eq. 1)}$$

$$\text{Fe(III)-CBS} + e^- \rightarrow \text{Fe(II)-CBS} \quad \text{(Eq. 2)}$$

$$NO^\bullet + \text{Fe(II)-CBS} \rightleftharpoons \text{Fe(II)NO•-CBS} \quad \text{(Eq. 3)}$$

This reaction sequence implies that the ferric heme, once formed, should be reduced back to the ferrous state to react with NO• to form Fe(II)NO•-CBS. Accordingly, when the concentration of dithionite was lower than CBS so that the reductant was limiting, Fe(III)-CBS was the final product, and Fe(II)NO•-CBS formation was not detected (Fig. 1*B*). The reaction of ferric CBS with NO• is very slow as reported previously (32) and not expected to be a contributing factor under our experimental conditions.

An effect of dithionite on the reaction of Fe(II)-CBS with nitrite was observed. The time course of the reaction changed when the concentration of dithionite increased from 75 μM to 3.0 mM (Fig. 1*C*). A likely explanation for this observation is interference from the reaction between NO• and dithionite ($k = \sim 1.4 \times 10^3\ M^{-1}\ s^{-1}$) (48). Computer-assisted simulations were performed using the reactions and rate constants listed in Table 1, and initial concentrations of the reagents, Fe(II)-CBS, dithionite, and nitrite as used in the experiments. Although the experimental and simulated results were not identical, the simulations provided insights into the reaction kinetics. The interference of dithionite in the reaction was revealed by exclusion of the direct reaction between dithionite and NO• from the

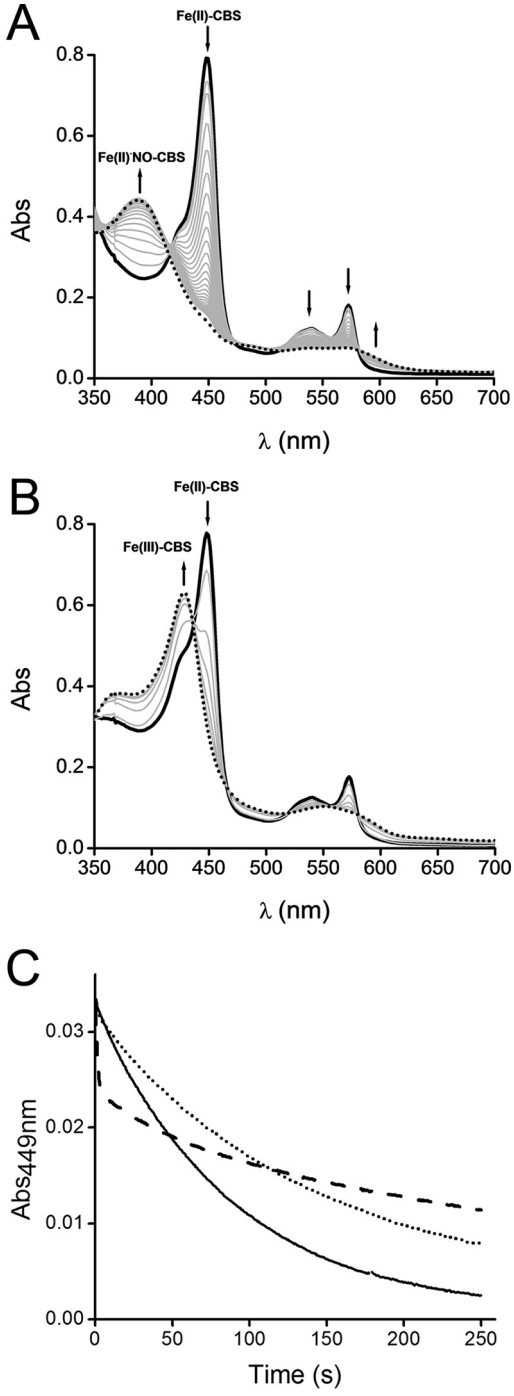

FIGURE 1. **Effect of dithionite concentration on Fe(II)-CBS reaction with nitrite.** *A*, Fe(III)-CBS (10 μM) was reduced with dithionite (90 μM) in phosphate buffer (0.1 M, pH 7.4, with DTPA 0.1 mM) inside an anaerobic chamber. Then sodium nitrite (1 mM) was added, the cuvette was sealed, and UV-visible absorption spectra were recorded outside the anaerobic chamber immediately after mixing (*black trace*) and every minute (*gray traces*) for 35 min (*dotted trace*). The *arrows* indicate the direction of the absorbance change over time. *B*, Fe(III)-CBS (10 μM) was reduced with a substoichiometric dithionite concentration (8 μM) and a similar procedure as described above was then followed. Selected UV-visible absorption spectra recorded immediately after mixing (*black trace*); at 1, 2, 3, 4, and 5 min (*gray traces*); and at 12 min (*dotted trace*) are shown. *C*, an anaerobic solution of Fe(III)-CBS (5 μM) was reduced with dithionite (50 μM) and mixed with sodium nitrite (10 mM) in the presence of various dithionite concentrations in sodium phosphate buffer (0.1 M, pH 7.4, with 0.1 mM DTPA) at 37 °C. The *lines* represent the kinetic traces of Fe(II)-CBS decay at 449 nm obtained with different dithionite concentrations: 75 μM (*solid line*), 275 μM (*dotted line*), and 3.0 mM (*dashed line*). The concentrations are those after mixing. The experiments were repeated at least twice, and representative data are shown.

TABLE 1
Reactions involved in the anaerobic reaction of dithionite-reduced CBS with nitrite

Reaction	Rate constant[a]	References
$S_2O_4^{2-} \rightleftharpoons 2\ SO_2^{\bullet-}$	2.5 s^{-1} (f),[b] 1.8 × 10^9 M^{-1} s^{-1} (r)	Refs. 72 and 73
Fe(III)-CBS + $SO_2^{\bullet-} \rightarrow$ Fe(II)-CBS + SO_2	1.58 × 10^5 M^{-1} s^{-1}	Refs. 28 and 74
Fe(II)-CBS + $NO_2^- + H^+ \rightarrow$ Fe(III)-CBS + $NO^\bullet + OH^-$	0.66 M^{-1} s^{-1}	This work and Ref. 37
Fe(II)-CBS + $NO^\bullet \rightleftharpoons$ Fe(II)$NO^\bullet$-CBS	8 × 10^3 M^{-1} s^{-1} (f), 3 × 10^{-3} s^{-1} (r)	Ref. 32
$NO^\bullet + S_2O_4^{2-} \rightarrow$ products	1.4 × 10^3 M^{-1} s^{-1}	Ref. 48
Fe(II)-CBS + $HSO_3^-/SO_3^{2-} \rightarrow$ Fe(III)-CBS + $SO_2^{\bullet-} + OH^-$	17 M^{-1} s^{-1}	Ref. 32
$SO_2 + H_2O \rightleftharpoons HSO_3^-/SO_3^{2-} + H^+$	3.4 × 10^6 s^{-1} (f); 2.0 × 10^8 M^{-1} s^{-1} (r)	Ref. 75

[a] Rate constants are reported at pH 7.4 and 25 °C except for the homolysis of dithionite, at pH 6.5 (72, 73) and for the reaction of Fe(II)-CBS with nitrite, reported at 37 °C (this work). For simulations, the rate constants at 25 °C were multiplied by 2.
[b] (f) and (r) represent forward and reverse kinetic constants, respectively.

simulation (Fig. 2, *A* and *B*). It is important to note that dithionite does not effectively reduce nitrite (49). Dithionite can compete with Fe(II)-CBS for $NO^\bullet$ because the formation of Fe(II)$NO^\bullet$-CBS is a relatively slow process (32). Accordingly, when a 10-fold higher value for the k_{on} for the reaction between Fe(II)-CBS and $NO^\bullet$ was used in the simulation, the interference due to dithionite decreased (Fig. 2*C*).

To minimize the interference of dithionite, the kinetics of Fe(II)-CBS reaction with nitrite and Fe(II)$NO^\bullet$-CBS formation were further characterized using relatively low dithionite concentrations (~10–15 μM) but in excess over CBS. In the UV-visible spectra, clear isosbestic points were observed at 410 and 587 nm up to 300 s (Fig. 3*A*). At longer times, the isosbestics were lost, and the absorbance at 394 nm decayed slowly. The Fe(III)-CBS intermediate was not detected because it is reduced back to Fe(II)-CBS by dithionite. Using the rate constants shown in Table 1, kinetic simulations showed that during the time course of the reaction, the concentration of Fe(III)-CBS would remain low, representing <10% of total CBS, whereas the decay of Fe(II)-CBS is paralleled by an increase in Fe(II)$NO^\bullet$-CBS. The reaction course during the first 300 s monitored by the decay of the signal at 449 nm characteristic of Fe(II)-CBS or that at 394 nm because of formation of Fe(II)$NO^\bullet$-CBS were fitted to a single exponential plus straight line function (Fig. 3*A*, *inset*). The observed rate constants at 449 nm increased linearly with nitrite concentration, showing no evidence of saturation behavior up to 50 mM nitrite (Fig. 3*B*). From the slope of the plot, the second order rate constant for full-length CBS was estimated to be 0.66 ± 0.03 M^{-1} s^{-1} at pH 7.4 and 37 °C. This value for the second order rate constant between nitrite and Fe(II)-CBS is an approximation because of the multiple reactions required to obtain Fe(II)$NO^\bullet$-CBS from Fe(II)-CBS and nitrite. In the presence of the allosteric activator AdoMet, the second order rate constant obtained from fits at 449 nm is 1.32 ± 0.06 M^{-1} s^{-1}, ~2-fold greater than in its absence and in agreement with a previous report (37). Interestingly, the T257I mutant of CBS exhibited a >10-fold increase in the value of the second order rate constant than wild-type CBS in the absence of AdoMet (Table 2). For truncated CBS, we also determined a higher reactivity with nitrite compared with full-length CBS, with estimates for the second order rate constant of 2.37 ± 0.07 M^{-1} s^{-1}.

Kinetics of Fe(II)$NO^\bullet$-CBS Reaction with O_2—As reported previously, air exposure of Fe(II)$NO^\bullet$-CBS results in reoxidation to Fe(III)-CBS concomitant with recovery of enzyme activity (32, 37). When a solution of Fe(II)$NO^\bullet$-CBS was mixed with excess O_2, the nitrosylated enzyme with the characteristic absorption peak at 394 nm slowly converted to Fe(III)-CBS with a maximum at 428 nm (Fig. 4*A*). Clear isosbestic points were not observed in the UV-visible spectra. The increase in absorbance at 428 nm was biphasic and fitted a double exponential function (Fig. 4*B*, *inset*). The first phase had k_{obs} values on the order of 10^{-3} s^{-1} that depended linearly on oxygen concentration, leading to an apparent second order rate constant of 2.0 ± 0.4 M^{-1} s^{-1}. The second phase had a k_{obs} value of ~2 × 10^{-4} s^{-1} and was constant within the range of O_2 concentrations (Fig. 4*B*). In some experiments, an initial fast phase could be detected. This kinetic phase has been reported previously (32) but presented high variability and was not pursued further. It is possible that this fast phase was due to the presence of a small amount of reduced CBS without bound $NO^\bullet$ that auto-oxidized quickly upon oxygenation. Under anaerobic conditions, Fe(II)$NO^\bullet$-CBS decayed spontaneously but extremely slowly to the ferric species, with a half-life of ~11 h at room temperature (data not shown).

Peroxynitrite Formation by Fe(II)$NO^\bullet$-CBS Exposed to O_2—The formation of peroxynitrite was evaluated using the boronate probe CBA, which reacts fast with peroxynitrite (k = 1.1 × 10^6 M^{-1} s^{-1}) to yield COH as the major product, which can be followed by fluorescence spectroscopy (42). As shown in Fig. 5*A*, upon exposure of Fe(II)$NO^\bullet$-CBS to O_2 in the presence of CBA, an increase in fluorescence intensity over time corresponding to COH accumulation was observed, indicating peroxynitrite formation. The kinetics of peroxynitrite formation were relatively slow and, with a global k_{obs} of (1.5 ± 0.4) × 10^{-3} s^{-1}, mirrored the kinetics of Fe(II)$NO^\bullet$-CBS decay to Fe(III)-CBS (0.8–2.8 × 10^{-3} s^{-1}). Controls lacking CBS did not result in significant COH formation. Artifacts derived from reactions of dithionite were avoided by passing the Fe(II)$NO^\bullet$-CBS solution over a gel filtration column before CBA addition and O_2 exposure. Furthermore, photochemical artifacts were minimized by reducing the slit width and by taking measurements every 10 min rather than continuous exposure of the sample to incident light. The presence of catalase did not alter the yield of COH, confirming that H_2O_2 is not involved in its formation, which is consistent with the much greater rate constant for the reaction of catalase (0.1 μM) with H_2O_2 (~10^7 M^{-1} s^{-1}) *versus* CBA (20 μM) with H_2O_2 (1.5 M^{-1} s^{-1}). In the presence of superoxide dismutase (5.5 μM), which reacts with $O_2^{\bullet-}$ with a rate constant of 2 × 10^9 M^{-1} s^{-1} (50), COH fluorescence was partially inhibited (~ 40%). The inhibition increased further to ~60%, in the presence of both superoxide dismutase and catalase. This is expected because catalase reacts with the H_2O_2 formed from superoxide dismutase-catalyzed dispro-

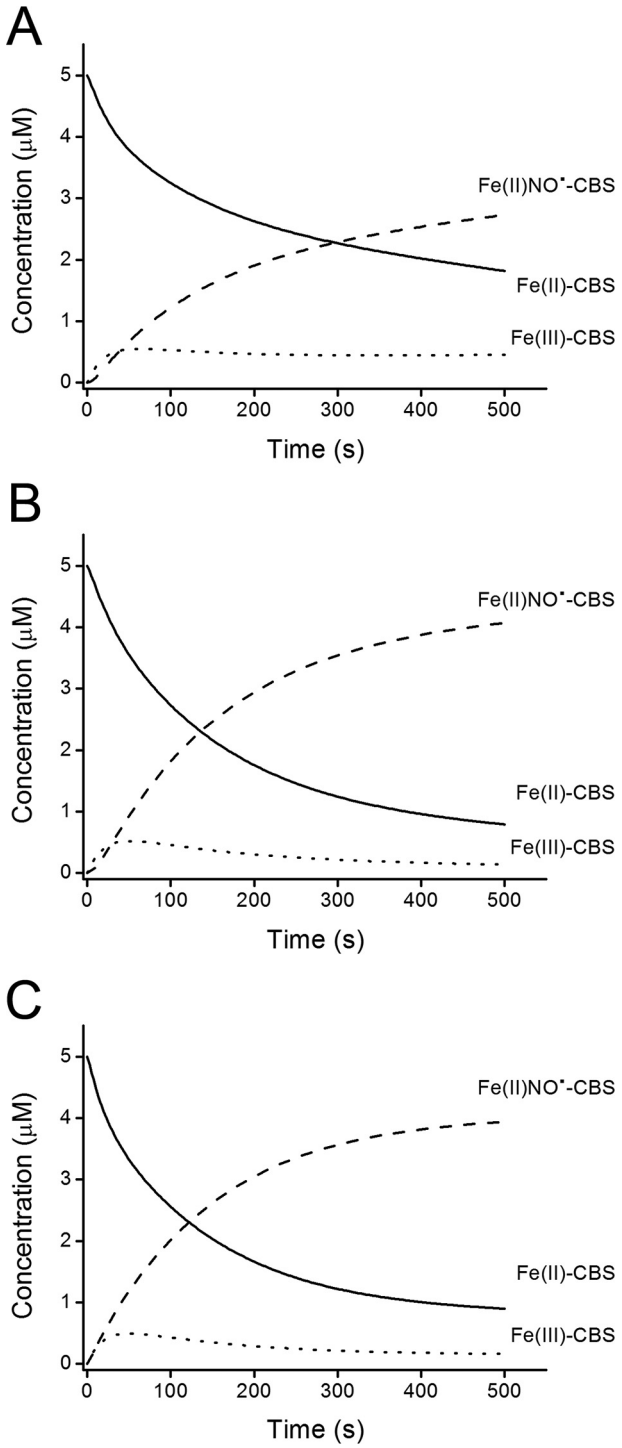

FIGURE 2. **Simulated profile of Fe(II)-CBS reaction with nitrite.** Computer-assisted simulations of the transient concentrations of Fe(II)-CBS (*solid line*), Fe(III)-CBS (*dotted line*), and Fe(II)NO•-CBS (*dashed line*). Simulations were performed using as initial concentrations of Fe(II)-CBS, dithionite, and nitrite 5 μM, 15 μM, and 10 mM, respectively. *A*, simulation obtained using the reactions and rate constants listed in Table 1. *B*, simulations obtained when the direct reaction between dithionite and NO• was omitted from the list of reactions. *C*, simulation obtained when the reaction between dithionite and NO• was included, but a 10-fold higher k_{on} value for NO• binding to Fe(II)-CBS was used.

portionation of $O_2^{\bullet-}$. Taken together, the results suggest that diffusible $O_2^{\bullet-}$ is implicated in the formation of most but not all peroxynitrite.

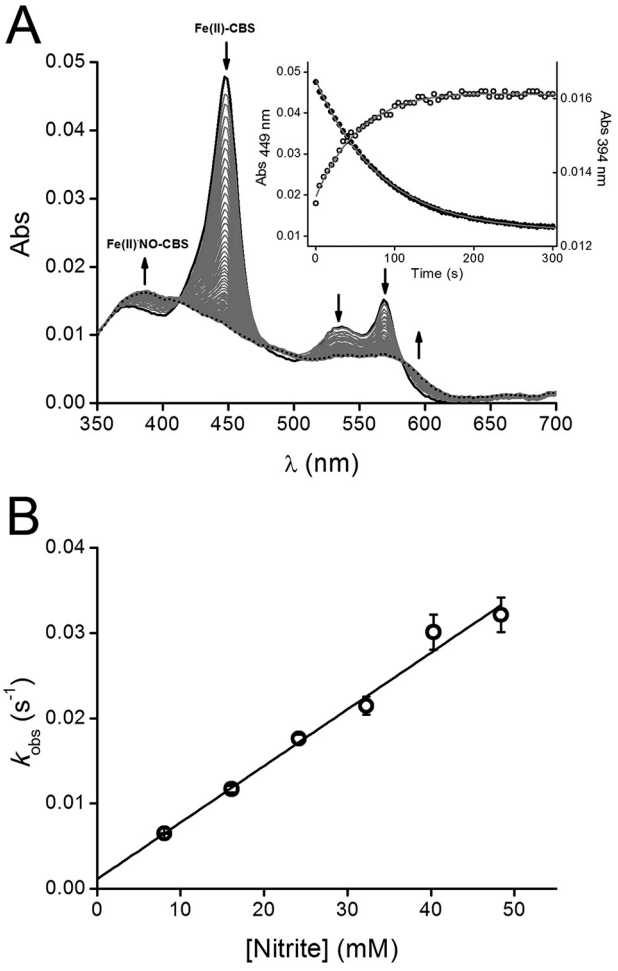

FIGURE 3. **Kinetics of Fe(II)-CBS reaction with nitrite.** *A*, UV-visible absorption spectra obtained in a stopped flow instrument after mixing full-length CBS (reduced with dithionite) with sodium nitrite in phosphate buffer (0.1 M, pH 7.4, 0.1 mM DTPA) at 37 °C. The concentrations of CBS, dithionite, and nitrite after mixing were 1 μM, ~10 μM, and 10 mM, respectively. Spectra were collected from 0.5 to 500 s every 0.5 s. For clarity, only selected spectra are shown. The *arrows* indicate the direction of the absorbance change over time. *Inset*, absorbance at 394 nm (*open circles*) and 449 nm (*closed circles*) were plotted against time up to 300 s. The *solid lines* represent the fits to single exponential plus a straight line functions. *B*, an anaerobic solution of Fe(III)-CBS (5 μM) in phosphate buffer (0.1 M, pH 7.4, 0.1 mM DTPA) was reduced with low dithionite concentrations (15 μM). The resulting Fe(II)-CBS solution was then mixed with increasing sodium nitrite concentrations. The absorbance at 449 nm was recorded outside the anaerobic chamber at 37 °C and fitted to a single exponential plus straight line function to obtain the observed rate constants (k_{obs}). The results are represented as the means ± standard deviation ($n \geq 3$).

TABLE 2

Comparison of reaction rate constants of mammalian hemeproteins with nitrite

Mammalian hemeproteins	Rate constant[a]	References
	$M^{-1}\,s^{-1}$	
CBS full length	0.66 ± 0.03	This work and Ref. 37
CBS full length + AdoMet	1.32 ± 0.06	This work
CBS full length T257I	7.70 ± 0.62[b]	This work
CBS truncated	2.37 ± 0.07	This work
Hemoglobin (human, T state)	0.12	Ref. 76
Hemoglobin (human, R state)	6	Ref. 76
Myoglobin (horse)	2.9	Ref. 47
Neuroglobin (human)	0.26	Ref. 47
Cytoglobin (human)	0.14	Ref. 77

[a] Rate constants reported at pH 7.4 and 37 °C, except for myoglobin and cytoglobin reported at pH 7 and 25 °C.
[b] Rate constant was determined at 394 nm.

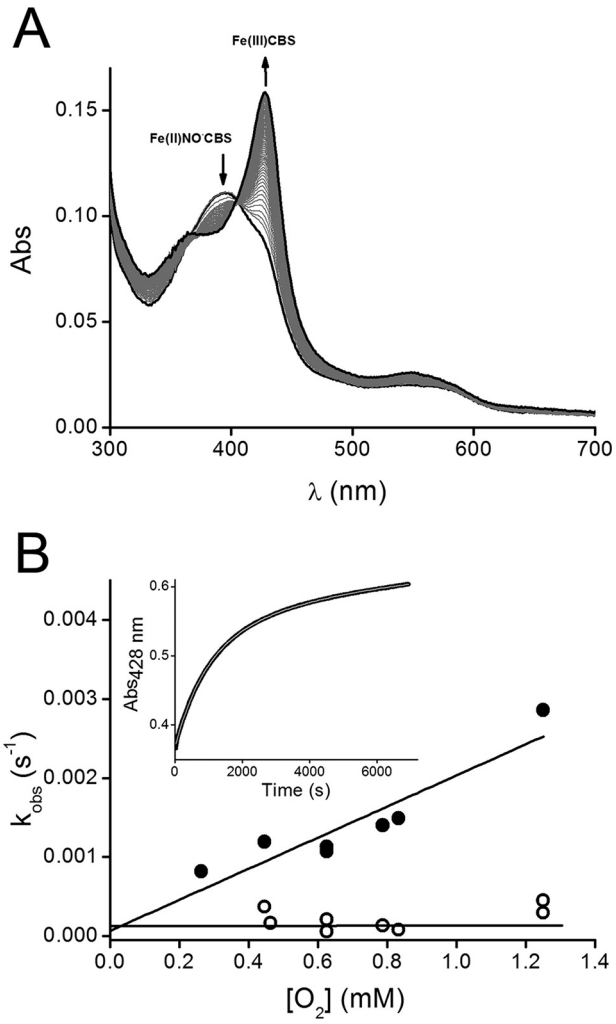

FIGURE 4. **Oxidation of Fe(II)NO·-CBS by O_2.** *A*, an anaerobic solution of Fe(III)-CBS (40 μM) was reduced with dithionite (200 μM) and mixed with sodium nitrite (4 mM) in phosphate buffer (0.1 M, pH 7.4, with 0.1 mM DTPA) inside the anaerobic chamber. The resulting solution was gel-filtered to remove excess dithionite and nitrite, and after removing the sample from the chamber, Fe(II)NO·-CBS was mixed with an equal volume of a solution containing O_2 obtained by equilibrating buffer with 100% O_2 (final concentration, 50% O_2, ~0.625 mM). The cuvette headspace was also bubbled with 50% O_2. UV-visible absorption spectra were registered every 4 min up to 250 min at 25 °C. *B*, an anaerobic solution of Fe(III)-CBS (10 μM) was reduced with dithionite (90 μM) in phosphate buffer (0.1 M, pH 7.4, with DTPA 0.1 mM) inside the anaerobic chamber. Then sodium nitrite (1 mM) was added, and after removing the sample from the anaerobic chamber, the resulting Fe(II)NO·-CBS solution was bubbled ~1 min with 100% O_2 (1.25 mM), air (21% O_2) or mixed with solutions of increased O_2 concentrations obtained from mixing known volumes of anaerobic and O_2-equilibrated water at 25 °C. The k_{obs} (s^{-1}) values, determined from the fit of the increase of Fe(III)-CBS at 428 nm to a double exponential function, were plotted against O_2 concentrations (0.263–1.25 mM) for the first (*closed circles*) and second (*open circles*) phases at each O_2 concentration. *Inset*, kinetic trace of the reaction monitored by the increase of absorbance at 428 nm. The *line* represents the best fit to double exponential function. The experiment was repeated at least three times, and representative data are shown.

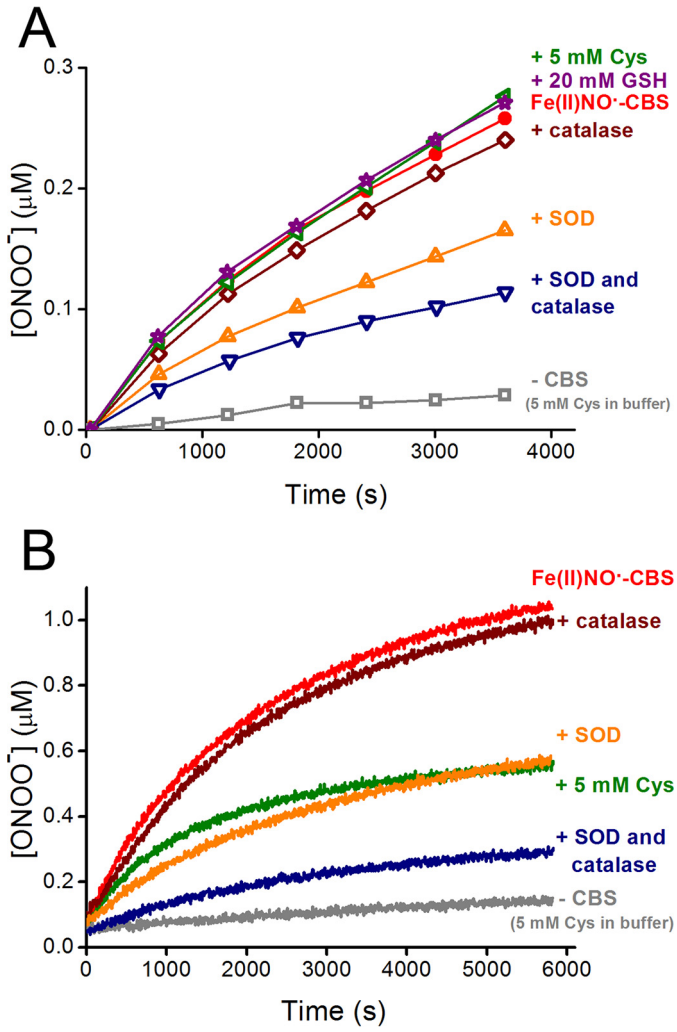

FIGURE 5. **Detection of peroxynitrite produced by reaction of Fe(II)NO·-CBS with O_2 in the presence of CBA.** An anaerobic solution of Fe(III)-CBS (15 μM) was reduced with dithionite (100 μM) and mixed with sodium nitrite (4 mM) in phosphate buffer (0.1 M, pH 7.4, with 0.1 mM DTPA). After 60 min, the solution of Fe(II)NO·-CBS was purified using a gel filtration column and mixed with CBA and water-equilibrated with O_2 (100%). The final concentrations were ~7.5, 20, and 625 μM for Fe(II)NO·-CBS, CBA, and O_2, respectively. The same procedure was repeated in the presence of cysteine (5 mM), glutathione (20 mM), catalase (0.1 μM), superoxide dismutase (*SOD*, 5.5 μM), and both superoxide dismutase and catalase. A control lacking CBS, containing cysteine (5 mM) in buffer was also included. *A*, the increase in the fluorescence intensity emission corresponding to COH formation was recorded every 10 min at 25 °C (λ_{ex} = 330 nm, λ_{em} = 450 nm) to minimize the incident light. *B*, the same procedure as described above, but the fluorescence intensity emission was recorded continuously to 6000 s. The experiment was repeated at least three times, and representative data are shown.

In the presence of 20 mM glutathione or 5 mM cysteine, which scavenge peroxynitrite with rate constants of 6×10^2 M^{-1} s^{-1} and 3.5×10^3 M^{-1} s^{-1}, respectively, at 25 °C and pH 7.4 (51, 52), COH formation was not inhibited (Fig. 5*A*). Controls showed that COH fluorescence observed with cysteine alone was negligible and that cysteine and glutathione, at the mentioned concentrations, inhibited COH fluorescence from authentic peroxynitrite to ~52 and 60%, respectively, as expected from kinetic considerations. Thus, the lack of inhibition by cysteine and glutathione in the case of Fe(II)NO·-CBS supports the possibility that the peroxynitrite formed was nitrogen-bound to the heme in CBS and was able to perform a nucleophilic attack of the terminal peroxidatic oxygen on boron but was unable to react with thiols as an electrophile. In contrast, when fluorescence was continuously recorded instead of being measured every 10 min, an inhibitory effect (~45%) of cysteine on COH formation was observed (Fig. 5*B*). This is likely to have been triggered by a photochemically induced dissociation of NO·

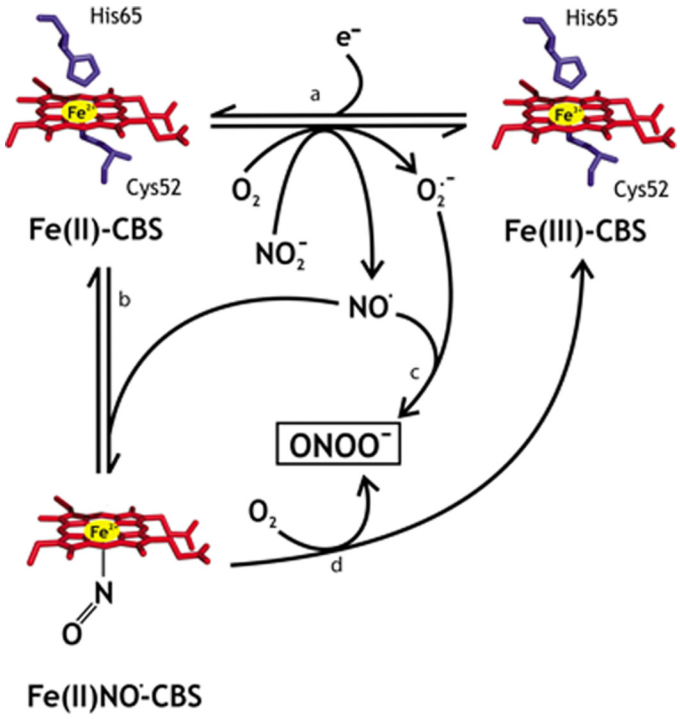

SCHEME 1. **Interaction of human CBS with nitrite.**

from Fe(II)NO•-CBS, leading to peroxynitrite formation in the presence of $O_2^{\bullet-}$.

Discussion

In the present study, we have characterized the kinetics of nitrite reduction by Fe(II)-CBS that leads to formation of Fe(II)NO•-CBS (pathways *a* and *b* in Scheme 1). We found that the dithionite concentration can affect the process of nitrite reduction by CBS. However, dithionite has been used at millimolar concentrations with other hemeproteins, apparently without this complication. We attribute this difference to the fact that other ferrous proteins such as hemoglobin, myoglobin, and neuroglobin react with NO• very fast and form very tight complexes, with k_{on} values $\sim 10^7$–10^8 M^{-1} s^{-1} and k_{off} values of $\sim 10^{-4}$ s^{-1} (53, 54). In contrast, Fe(II)-CBS reacts several orders of magnitude more slowly with NO•, with a k_{on} of 8×10^3 M^{-1} s^{-1} and k_{off} of 3×10^{-3} s^{-1} (32). Thus, hemoglobin, myoglobin, and neuroglobin are able to outcompete high dithionite concentrations and efficiently scavenge the NO• formed, whereas CBS cannot, necessitating the use of lower dithionite concentration in our experiments.

The second order rate constant for the reaction of nitrite and Fe(II)-CBS obtained with full-length CBS was estimated to be 0.66 ± 0.03 M^{-1} s^{-1} at pH 7.4 and 37 °C. This value, which represents an approximation of the rate constant, is higher than those of several hemeproteins that function as nitrite reductases including hemoglobin (T state), neuroglobin, and cytoglobin (Table 2). In addition, Fe(II)-CBS binds NO• more loosely than other hemeproteins ($K_d = \sim 0.23$ μM (32)). This looser binding means that the NO• formed from nitrite reduction would be available to react with potential targets instead of remaining bound to CBS. Together with the relatively high rate constant for nitrite reduction, the low affinity for NO• suggests that CBS could be a potential source of NO• *in vivo*. The increased rate constants for the full-length CBS in the presence of the allosteric activator AdoMet and for the truncated variant lacking the AdoMet binding domain suggest that the regulatory domain affects the heme environment. In this regard, it has recently been reported that AdoMet binding enhances association of CO and, to a lesser extent, NO•, to Fe(II)-CBS (55). Remarkably, the mutant T257I CBS exhibited enhanced nitrite reduction kinetics. Mutations at this conserved threonine residue located in the PLP binding pocket drastically affect enzyme activity (24). A pathogenic T257M mutation has been described in a homocystinuric patient (56). In addition, these mutations at Thr^{257} perturb the heme environment, as observed by the enhanced propensity to form the Fe(II)424-CBS species (15, 24) and, as shown herein, for T257I to enhance reduction of nitrite and generation of NO•.

From a mechanistic point of view, reduction of nitrite by six-coordinate Fe(II)-CBS could involve an outer sphere mechanism. Consistent with this possibility is the observation that dissociation of the cysteine ligand to heme does not appear to limit Fe(II)-NO•-CBS formation because plots of k_{obs} *versus* nitrite concentration are linear up to 50 mM nitrite. Furthermore, the k_{obs} values for Fe(II)-NO•-CBS formation (0.006–0.032 s^{-1}; Fig. 3*B*) are similar to or higher than the values for dissociation of the cysteine ligand, which was estimated from the maximum rate constant for CO binding to be ~ 0.0166 s^{-1} (31), 0.012 s^{-1} (32), and 0.0031 s^{-1} (28). The outer sphere proposal is further consistent with the very negative reduction potential of CBS (−0.350 V, (21)) that would favor electron transfer according to Marcus theory. As precedent, the reaction of Fe(II)-CBS with O_2, which occurs with a k_{obs} of 20–80 s^{-1} and depends linearly on O_2 concentration (30). Alternatively, the reaction with nitrite would implicate a pentacoordinate (pentacoordinate ferrous CBS) species. This has been proposed in the case of human neuroglobin, another hexacoordinate hemeprotein for which thorough kinetic analyses have been reported (47, 57). The first step of the reaction is the dissociation of an axial His ligand, followed by nitrite (or nitrous acid) binding to the ferrous iron, either through the nitrogen or the oxygen atoms. Proton addition and electron transfer occur, yielding ferric heme, NO•, and OH^-. Neuroglobin is a bis-His ligated protein with a reduction potential of −0.118 V; the dissociation of the axial His is estimated to occur at 0.4 s^{-1} (58), and the k_{obs} for the reaction with nitrite is $\sim$2 orders of magnitude lower (47) than this value. Thus, in the case of neuroglobin, it is likely that nitrite reduction is preceded by conversion to the pentacoordinate state. However, in the case of CBS, an outer sphere process seems to be the more probable pathway for explaining the reactivity of this unusual and low potential hemeprotein.

In contrast to the rapid monophasic O_2-mediated reoxidation of Fe(II)-CBS to Fe(III)-CBS (30), O_2-dependent reoxidation of Fe(II)NO•-CBS is slow and showed complex kinetic behavior with a biphasic time course and no clear isosbestic points. The results obtained for Fe(II)NO•-CBS can be interpreted in terms of two parallel mechanisms, one that involves the slow dissociation of NO• as a rate-limiting step (0.003 s^{-1} (32)) followed by a fast reaction with O_2 (1.11×10^5 M^{-1} s^{-1}

(30)), and another one with linear dependence on O_2 concentration in which O_2 first reacts with Fe(II)NO•-CBS, albeit slowly. Biphasic processes without isosbestic points have also been reported for the reactions of nitrosyl derivatives of myoglobin (59), hemoglobin (60), and neuroglobin (61) with O_2. In the case of myoglobin, both phases were slow (10^{-4} s^{-1}), and one of them showed hyperbolic dependence on O_2 concentration, whereas the other was independent. In the case of hemoglobin, the rate of ferric heme formation appeared limited by the dissociation of NO•, which occurred on a similar (10^{-4} s^{-1}) time scale. In the case of neuroglobin, the first phase depended linearly on O_2 concentration with a second order rate constant of 16 M^{-1} s^{-1}, and the second phase was independent of O_2 concentration with k_{obs} of 5×10^{-4} s^{-1}. In contrast, for the heme thiolate protein, nitric oxide synthase, the reaction of the Fe(II)NO• species with O_2 occurs through a rapid direct reaction, but in this case the hexacoordinate Fe(II)NO• complex is very different from the pentacoordinate one observed in CBS (62, 63). In this context, it is important to note that, unlike other hemeproteins (*e.g.* hemoglobin, myoglobin, bacterial flavohemoglobins (64)), typical nitric oxide dioxygenation is unlikely to occur in the case of CBS. Such a process would require the reaction of NO• with an oxyferrous Fe(II)O_2 heme to form nitrate and ferric heme. Fe(II)-CBS is unable to form a stable oxyferrous species (30), so typical nitric oxide dioxygenase activity can be excluded.

Our results with CBA demonstrate that peroxynitrite is formed during reoxidation of Fe(II)NO•-CBS. Although CBA can also react with H_2O_2 (1.5 M^{-1} s^{-1}) (42) and with amino acid hydroperoxides (7–23 M^{-1} s^{-1}) (65), the rate constants are several orders of magnitude smaller than with peroxynitrite ($k = 1.1 \times 10^6$ M^{-1} s^{-1}). Peroxynitrite formation is likely to be mediated by two parallel mechanisms that mirror the kinetics of O_2-dependent reoxidation of Fe(II)NO•-CBS. The first is mediated by dissociation of the precursor radical NO• followed by the fast reaction of Fe(II)-CBS with O_2 to form $O_2^{\bullet-}$ (pathway *c* in Scheme 1). NO• and $O_2^{\bullet-}$ would then react with a diffusion-limited rate constant of $\sim 10^{10}$ M^{-1} s^{-1}. The second is dependent on the direct reaction of O_2 with Fe(II)NO•-CBS (pathway *d* in Scheme 1). The fact that superoxide dismutase (in the presence of catalase to decompose the H_2O_2 formed) did not completely inhibit COH formation suggests that diffusible $O_2^{\bullet-}$ cannot account for all the peroxynitrite formed and that some peroxynitrite is generated directly at the heme site by reaction of O_2 with heme-bound NO•, generating a nitrogen-bound heme-peroxynitrite species. In addition, the observation that glutathione and cysteine, which are efficient peroxynitrite scavengers, did not inhibit formation of COH fluorescence is also consistent with the *in situ* formation of peroxynitrite at the heme site.

Fe(III)-CBS can be reduced to Fe(II)-CBS by a physiological reducing system (28, 29). Thus, in addition to being a source of $O_2^{\bullet-}$ by a fast reaction with O_2 (30), under low O_2 tension conditions, Fe(II)-CBS could react with nitrite leading to the transient formation of Fe(II)NO•-CBS. This process might constitute not only a mechanism for decreasing the yield of cystathionine, cysteine, and CBS-derived H_2S but also might represents a potential source of NO•. Moreover, O_2-mediated Fe(II)NO•-CBS reoxidation could provide a previously unrecognized source of peroxynitrite, a strong biological oxidizing and nitrating agent that can react with CO_2, thiols, selenium compounds, and metal centers (66–68). In addition, CBS is susceptible to peroxynitrite. We have previously reported that peroxynitrite reacts with Fe(III)-CBS with a second order rate constant of $(2.4–5.0) \times 10^4$ M^{-1} s^{-1} (pH 7.4 and 37 °C), leading to nitration of protein residues, loss of heme thiolate coordination, bleaching, and inactivation of the enzyme (26), with possible relevance to hyperhomocysteinemia and pathogenesis. Increased oxidative stress caused by CBS deficiency was reported to correlate with the development of liver disease (69). In addition, a decrease in CBS activity with elevation in homocysteine concentrations was observed to be associated with an increase in oxidative stress in rat kidney ischemia-reperfusion injury, and it was hypothesized that an increase in NO• levels during reperfusion might play a role in regulating CBS activity (70, 71). In summary, this study adds important new insights to our understanding of heme reactivity in CBS and adds to the evidence that CBS represents a point of interplay between nitrite, peroxynitrite, NO•, $O_2^{\bullet-}$, CO, and H_2S.

Author Contributions—S. C. designed, performed, and analyzed the experiments and wrote the manuscript. E. C. performed experiments and analyzed the data. C. G. and P. K. Y. helped conceive the experiments and contributed to analyze the data. D. P. B. provided technical assistance, analyzed the results, and edited the manuscript. B. A. and R. B. helped conceive the experiments, analyzed the data, and co-wrote the manuscript. All authors approved the final version of the manuscript.

Acknowledgments—We thank Drs. Gerardo Ferrer-Sueta and Matías Möller (Facultad de Ciencias, Universidad de la República, Uruguay); Stephen W. Ragsdale, Omer Kabil, Victor Vitvitsky, Dariusz Sliwa, and Tatyana Spolitak (Department of Biological Chemistry, University of Michigan, Ann Arbor); and Javier Seravalli (University of Nebraska, Lincoln) for helpful discussions and technical assistance.

References

1. Abe, K., and Kimura, H. (1996) The possible role of hydrogen sulfide as an endogenous neuromodulator. *J. Neurosci.* **16,** 1066–1071
2. Kabil, O., and Banerjee, R. (2010) Redox biochemistry of hydrogen sulfide. *J. Biol. Chem.* **285,** 21903–21907
3. Zhao, W., Zhang, J., Lu, Y., and Wang, R. (2001) The vasorelaxant effect of H_2S as a novel endogenous gaseous K_{ATP} channel opener. *EMBO J.* **20,** 6008–6016
4. Clarke, R., Smith, A. D., Jobst, K. A., Refsum, H., Sutton, L., and Ueland, P. M. (1998) Folate, vitamin B_{12}, and serum total homocysteine levels in confirmed Alzheimer disease. *Arch. Neurol.* **55,** 1449–1455
5. McCully, K. S. (1969) Vascular pathology of homocysteinemia: implications for the pathogenesis of arteriosclerosis. *Am. J. Pathol.* **56,** 111–128
6. Mills, J. L., McPartlin, J. M., Kirke, P. N., Lee, Y. J., Conley, M. R., Weir, D. G., and Scott, J. M. (1995) Homocysteine metabolism in pregnancies complicated by neural-tube defects. *Lancet* **345,** 149–151
7. Refsum, H., Ueland, P. M., Nygård, O., and Vollset, S. E. (1998) Homocysteine and cardiovascular disease. *Annu. Rev. Med.* **49,** 31–62
8. Kraus, J. P., Janosík, M., Kozich, V., Mandell, R., Shih, V., Sperandeo, M. P., Sebastio, G., de Franchis, R., Andria, G., Kluijtmans, L. A., Blom, H., Boers, G. H., Gordon, R. B., Kamoun, P., Tsai, M. Y., Kruger, W. D., Koch, H. G., Ohura, T., and Gaustadnes, M. (1999) Cystathionine β-synthase mutations in homocystinuria. *Hum. Mutat.* **13,** 362–375
9. Sen, S., and Banerjee, R. (2007) A pathogenic linked mutation in the catalytic core of human cystathionine β-synthase disrupts allosteric regula-

tion and allows kinetic characterization of a full-length dimer. *Biochemistry* **46,** 4110–4116
10. Kery, V., Poneleit, L., and Kraus, J. P. (1998) Trypsin cleavage of human cystathionine β-synthase into an evolutionarily conserved active core: structural and functional consequences. *Arch. Biochem. Biophys.* **355,** 222–232
11. Koutmos, M., Kabil, O., Smith, J. L., and Banerjee, R. (2010) Structural basis for substrate activation and regulation by cystathionine β-synthase (CBS) domains in cystathionine β-synthase. *Proc. Natl. Acad. Sci. U.S.A.* **107,** 20958–20963
12. Meier, M., Janosik, M., Kery, V., Kraus, J. P., and Burkhard, P. (2001) Structure of human cystathionine β-synthase: a unique pyridoxal 5′-phosphate-dependent heme protein. *EMBO J.* **20,** 3910–3916
13. Taoka, S., Widjaja, L., and Banerjee, R. (1999) Assignment of enzymatic functions to specific regions of the PLP-dependent heme protein cystathionine β-synthase. *Biochemistry* **38,** 13155–13161
14. Ojha, S., Hwang, J., Kabil, O., Penner-Hahn, J. E., and Banerjee, R. (2000) Characterization of the heme in human cystathionine β-synthase by x-ray absorption and electron paramagnetic resonance spectroscopies. *Biochemistry* **39,** 10542–10547
15. Taoka, S., Lepore, B. W., Kabil, O., Ojha, S., Ringe, D., and Banerjee, R. (2002) Human cystathionine β-synthase is a heme sensor protein. Evidence that the redox sensor is heme and not the vicinal cysteines in the CXXC motif seen in the crystal structure of the truncated enzyme. *Biochemistry* **41,** 10454–10461
16. Taoka, S., West, M., and Banerjee, R. (1999) Characterization of the heme and pyridoxal phosphate cofactors of human cystathionine β-synthase reveals nonequivalent active sites. *Biochemistry* **38,** 2738–2744
17. Cuevasanta, E., Carballal, S., Graña, M., and Alvarez, B. (2013) The redox properties of the unique heme in cystathionine β-synthase. *BioInorg. React. Mech.* **9,** 27–34
18. Singh, S., Madzelan, P., and Banerjee, R. (2007) Properties of an unusual heme cofactor in PLP-dependent cystathionine β-synthase. *Nat. Prod. Rep.* **24,** 631–639
19. Kabil, O., Toaka, S., LoBrutto, R., Shoemaker, R., and Banerjee, R. (2001) Pyridoxal phosphate binding sites are similar in human heme-dependent and yeast heme-independent cystathionine β-synthases: evidence from ^{31}P NMR and pulsed EPR spectroscopy that heme and PLP cofactors are not proximal in the human enzyme. *J. Biol. Chem.* **276,** 19350–19355
20. Evande, R., Ojha, S., and Banerjee, R. (2004) Visualization of PLP-bound intermediates in hemeless variants of human cystathionine β-synthase: evidence that lysine 119 is a general base. *Arch. Biochem. Biophys.* **427,** 188–196
21. Singh, S., Madzelan, P., Stasser, J., Weeks, C. L., Becker, D., Spiro, T. G., Penner-Hahn, J., and Banerjee, R. (2009) Modulation of the heme electronic structure and cystathionine β-synthase activity by second coordination sphere ligands: the role of heme ligand switching in redox regulation. *J. Inorg. Biochem.* **103,** 689–697
22. Smith, A. T., Su, Y., Stevens, D. J., Majtan, T., Kraus, J. P., and Burstyn, J. N. (2012) Effect of the disease-causing R266K mutation on the heme and PLP environments of human cystathionine β-synthase. *Biochemistry* **51,** 6360–6370
23. Weeks, C. L., Singh, S., Madzelan, P., Banerjee, R., and Spiro, T. G. (2009) Heme regulation of human cystathionine β-synthase activity: insights from fluorescence and Raman spectroscopy. *J. Am. Chem. Soc.* **131,** 12809–12816
24. Yadav, P. K., Xie, P., and Banerjee, R. (2012) Allosteric communication between the pyridoxal 5′-phosphate (PLP) and heme sites in the H2S generator human cystathionine β-synthase. *J. Biol. Chem.* **287,** 37611–37620
25. Vadon-Le Goff, S., Delaforge, M., Boucher, J. L., Janosik, M., Kraus, J. P., and Mansuy, D. (2001) Coordination chemistry of the heme in cystathionine β-synthase: formation of iron(II)-isonitrile complexes. *Biochem. Biophys. Res. Commun.* **283,** 487–492
26. Celano, L., Gil, M., Carballal, S., Durán, R., Denicola, A., Banerjee, R., and Alvarez, B. (2009) Inactivation of cystathionine β-synthase with peroxynitrite. *Arch. Biochem. Biophys.* **491,** 96–105
27. Taoka, S., Green, E. L., Loehr, T. M., and Banerjee, R. (2001) Mercuric chloride-induced spin or ligation state changes in ferric or ferrous human cystathionine β-synthase inhibit enzyme activity. *J. Inorg. Biochem.* **87,** 253–259
28. Carballal, S., Cuevasanta, E., Marmisolle, I., Kabil, O., Gherasim, C., Ballou, D. P., Banerjee, R., and Alvarez, B. (2013) Kinetics of reversible reductive carbonylation of heme in human cystathionine β-synthase. *Biochemistry* **52,** 4553–4562
29. Kabil, O., Weeks, C. L., Carballal, S., Gherasim, C., Alvarez, B., Spiro, T. G., and Banerjee, R. (2011) Reversible heme-dependent regulation of human cystathionine β-synthase by a flavoprotein oxidoreductase. *Biochemistry* **50,** 8261–8263
30. Carballal, S., Madzelan, P., Zinola, C. F., Graña, M., Radi, R., Banerjee, R., and Alvarez, B. (2008) Dioxygen reactivity and heme redox potential of truncated human cystathionine β-synthase. *Biochemistry* **47,** 3194–3201
31. Puranik, M., Weeks, C. L., Lahaye, D., Kabil, O., Taoka, S., Nielsen, S. B., Groves, J. T., Banerjee, R., and Spiro, T. G. (2006) Dynamics of carbon monoxide binding to cystathionine β-synthase. *J. Biol. Chem.* **281,** 13433–13438
32. Vicente, J. B., Colaço, H. G., Mendes, M. I., Sarti, P., Leandro, P., and Giuffrè, A. (2014) NO* binds human cystathionine β-synthase quickly and tightly. *J. Biol. Chem.* **289,** 8579–8587
33. Ingi, T., Chiang, G., and Ronnett, G. V. (1996) The regulation of heme turnover and carbon monoxide biosynthesis in cultured primary rat olfactory receptor neurons. *J. Neurosci.* **16,** 5621–5628
34. Taoka, S., and Banerjee, R. (2001) Characterization of NO binding to human cystathionine β-synthase: possible implications of the effects of CO and NO binding to the human enzyme. *J. Inorg. Biochem.* **87,** 245–251
35. Cherney, M. M., Pazicni, S., Frank, N., Marvin, K. A., Kraus, J. P., and Burstyn, J. N. (2007) Ferrous human cystathionine β-synthase loses activity during enzyme assay due to a ligand switch process. *Biochemistry* **46,** 13199–13210
36. Pazicni, S., Cherney, M. M., Lukat-Rodgers, G. S., Oliveriusová, J., Rodgers, K. R., Kraus, J. P., and Burstyn, J. N. (2005) The heme of cystathionine β-synthase likely undergoes a thermally induced redox-mediated ligand switch. *Biochemistry* **44,** 16785–16795
37. Gherasim, C., Yadav, P. K., Kabil, O., Niu, W. N., and Banerjee, R. (2014) Nitrite reductase activity and inhibition of H_2S biogenesis by human cystathionine ss-synthase. *PLoS One* **9,** e85544
38. Hughes, M. N., and Nicklin, H. G. (1968) The chemistry of pernitrites: part I. kinetics of decomposition of pernitrous acid. *J. Chem. Soc.* **A**, 450–452
39. Taoka, S., Ohja, S., Shan, X., Kruger, W. D., and Banerjee, R. (1998) Evidence for heme-mediated redox regulation of human cystathionine β-synthase activity. *J. Biol. Chem.* **273,** 25179–25184
40. Bradford, M. M. (1976) A rapid and sensitive method for the quantitation of microgram quantities of protein utilizing the principle of protein-dye binding. *Anal. Biochem.* **72,** 248–254
41. Schellenberg, K. A., and Hellerman, L. (1958) Oxidation of reduced diphosphopyridine nucleotide. *J. Biol. Chem.* **231,** 547–556
42. Zielonka, J., Sikora, A., Joseph, J., and Kalyanaraman, B. (2010) Peroxynitrite is the major species formed from different flux ratios of co-generated nitric oxide and superoxide: direct reaction with boronate-based fluorescent probe. *J. Biol. Chem.* **285,** 14210–14216
43. Mendes, P. (1993) Gepasi: a software package for modelling the dynamics, steady states and control of biochemical and other systems. *Comput. Appl. Biosci.* **9,** 563–571
44. Doyle, M. P., Pickering, R. A., DeWeert, T. M., Hoekstra, J. W., and Pater, D. (1981) Kinetics and mechanism of the oxidation of human deoxyhemoglobin by nitrites. *J. Biol. Chem.* **256,** 12393–12398
45. Gladwin, M. T., Grubina, R., and Doyle, M. P. (2009) The new chemical biology of nitrite reactions with hemoglobin: R-state catalysis, oxidative denitrosylation, and nitrite reductase/anhydrase. *Acc Chem. Res.* **42,** 157–167
46. Petersen, M. G., Dewilde, S., and Fago, A. (2008) Reactions of ferrous neuroglobin and cytoglobin with nitrite under anaerobic conditions. *J. Inorg. Biochem.* **102,** 1777–1782
47. Tiso, M., Tejero, J., Basu, S., Azarov, I., Wang, X., Simplaceanu, V., Frizzell, S., Jayaraman, T., Geary, L., Shapiro, C., Ho, C., Shiva, S., Kim-Shapiro, D. B., and Gladwin, M. T. (2011) Human neuroglobin functions as a redox-

regulated nitrite reductase. *J. Biol. Chem.* **286,** 18277–18289
48. Moore, E. G., and Gibson, Q. H. (1976) Cooperativity in the dissociation of nitric oxide from hemoglobin. *J. Biol. Chem.* **251,** 2788–2794
49. Grubina, R., Basu, S., Tiso, M., Kim-Shapiro, D. B., and Gladwin, M. T. (2008) Nitrite reductase activity of hemoglobin S (sickle) provides insight into contributions of heme redox potential versus ligand affinity. *J. Biol. Chem.* **283,** 3628–3638
50. Klug, D., Rabani, J., and Fridovich, I. (1972) A direct demonstration of the catalytic action of superoxide dismutase through the use of pulse radiolysis. *J. Biol. Chem.* **247,** 4839–4842
51. Koppenol, W. H., Moreno, J. J., Pryor, W. A., Ischiropoulos, H., and Beckman, J. S. (1992) Peroxynitrite, a cloaked oxidant formed by nitric oxide and superoxide. *Chem. Res. Toxicol.* **5,** 834–842
52. Zeida, A., González Lebrero, M. C., Radi, R., Trujillo, M., and Estrin, D. A. (2013) Mechanism of cysteine oxidation by peroxynitrite: An integrated experimental and theoretical study. *Arch. Biochem. Biophys.* **539,** 81–86
53. Quillin, M. L., Li, T., Olson, J. S., Phillips, G. N., Jr., Dou, Y., Ikeda-Saito, M., Regan, R., Carlson, M., Gibson, Q. H., Li, H., and Elber, R. (1995) Structural and functional effects of apolar mutations of the distal valine in myoglobin. *J. Mol. Biol.* **245,** 416–436
54. Van Doorslaer, S., Dewilde, S., Kiger, L., Nistor, S. V., Goovaerts, E., Marden, M. C., and Moens, L. (2003) Nitric oxide binding properties of neuroglobin: a characterization by EPR and flash photolysis. *J. Biol. Chem.* **278,** 4919–4925
55. Vicente, J. B., Colaço, H. G., Sarti, P., Leandro, P., and Giuffrè, A. (2016) *S*-Adenosyl-L-methionine modulates CO and NO* binding to the human H_2S-generating enzyme cystathionine β-synthase. *J. Biol. Chem.* **291,** 572–581
56. Sebastio, G., Sperandeo, M. P., Panico, M., de Franchis, R., Kraus, J. P., and Andria, G. (1995) The molecular basis of homocystinuria due to cystathionine β-synthase deficiency in Italian families, and report of four novel mutations. *Am. J. Hum. Genet.* **56,** 1324–1333
57. Tejero, J., Sparacino-Watkins, C. E., Ragireddy, V., Frizzell, S., and Gladwin, M. T. (2015) Exploring the mechanisms of the reductase activity of neuroglobin by site-directed mutagenesis of the heme distal pocket. *Biochemistry* **54,** 722–733
58. Brunori, M., Giuffrè, A., Nienhaus, K., Nienhaus, G. U., Scandurra, F. M., and Vallone, B. (2005) Neuroglobin, nitric oxide, and oxygen: functional pathways and conformational changes. *Proc. Natl. Acad. Sci. U.S.A.* **102,** 8483–8488
59. Møller, J. K., and Skibsted, L. H. (2004) Mechanism of nitrosylmyoglobin autoxidation: temperature and oxygen pressure effects on the two consecutive reactions. *Chemistry* **10,** 2291–2300
60. Herold, S., and Röck, G. (2005) Mechanistic studies of the oxygen-mediated oxidation of nitrosylhemoglobin. *Biochemistry* **44,** 6223–6231
61. Herold, S., Fago, A., Weber, R. E., Dewilde, S., and Moens, L. (2004) Reactivity studies of the Fe(III) and Fe(II)NO forms of human neuroglobin reveal a potential role against oxidative stress. *J. Biol. Chem.* **279,** 22841–22847
62. Hannibal, L., Somasundaram, R., Tejero, J., Wilson, A., and Stuehr, D. J. (2011) Influence of heme-thiolate in shaping the catalytic properties of a bacterial nitric-oxide synthase. *J. Biol. Chem.* **286,** 39224–39235
63. Tejero, J., Santolini, J., and Stuehr, D. J. (2009) Fast ferrous heme-NO oxidation in nitric oxide synthases. *FEBS J.* **276,** 4505–4514
64. Gardner, P. R. (2005) Nitric oxide dioxygenase function and mechanism of flavohemoglobin, hemoglobin, myoglobin and their associated reductases. *J. Inorg. Biochem.* **99,** 247–266
65. Michalski, R., Zielonka, J., Gapys, E., Marcinek, A., Joseph, J., and Kalyanaraman, B. (2014) Real-time measurements of amino acid and protein hydroperoxides using coumarin boronic acid. *J. Biol. Chem.* **289,** 22536–22553
66. Carballal, S., Bartesaghi, S., and Radi, R. (2014) Kinetic and mechanistic considerations to assess the biological fate of peroxynitrite. *Biochim. Biophys. Acta* **1840,** 768–780
67. Ferrer-Sueta, G., and Radi, R. (2009) Chemical biology of peroxynitrite: kinetics, diffusion, and radicals. *ACS Chem. Biol.* **4,** 161–177
68. Radi, R. (2013) Peroxynitrite, a stealthy biological oxidant. *J. Biol. Chem.* **288,** 26464–26472
69. Robert, K., Nehmé, J., Bourdon, E., Pivert, G., Friguet, B., Delcayre, C., Delabar, J. M., and Janel, N. (2005) Cystathionine β synthase deficiency promotes oxidative stress, fibrosis, and steatosis in mice liver. *Gastroenterology* **128,** 1405–1415
70. Prathapasinghe, G. A., Siow, Y. L., and O, K. (2007) Detrimental role of homocysteine in renal ischemia-reperfusion injury. *Am. J. Physiol. Renal Physiol.* **292,** F1354–F1363
71. Prathapasinghe, G. A., Siow, Y. L., Xu, Z., and O, K. (2008) Inhibition of cystathionine-β-synthase activity during renal ischemia-reperfusion: role of pH and nitric oxide. *Am. J. Physiol. Renal Physiol.* **295,** F912–F922
72. Creutz, C., and Sutin, N. (1974) Kinetics of the reactions of sodium dithionite with dioxygen and hydrogen peroxide. *Inorg. Chem.* **13,** 2041–2043
73. Lambeth, D. O., and Palmer, G. (1973) The kinetics and mechanism of reduction of electron transfer proteins and other compounds of biological interest by dithionite. *J. Biol. Chem.* **248,** 6095–6103
74. Carballal, S., Cuevasanta, E., Marmisolle, I., Kabil, O., Gherasim, C., Ballou, D. P., Banerjee, R., and Alvarez, B. (2016) Correction to kinetics of reversible reductive carbonylation of heme in human cystathionine β-synthase. *Biochemistry* **55,** 238
75. Schwartz, S. E., and Freiberg, J. E. (1981) Mass-transport limitation to the rate of reaction of gases in liquid droplets: application to oxidation of SO_2 in aqueous solutions. *Atmos. Environ.* **15,** 1129–1144
76. Huang, Z., Shiva, S., Kim-Shapiro, D. B., Patel, R. P., Ringwood, L. A., Irby, C. E., Huang, K. T., Ho, C., Hogg, N., Schechter, A. N., and Gladwin, M. T. (2005) Enzymatic function of hemoglobin as a nitrite reductase that produces NO under allosteric control. *J. Clin. Invest.* **115,** 2099–2107
77. Li, H., Hemann, C., Abdelghany, T. M., El-Mahdy, M. A., and Zweier, J. L. (2012) Characterization of the mechanism and magnitude of cytoglobin-mediated nitrite reduction and nitric oxide generation under anaerobic conditions. *J. Biol. Chem.* **287,** 36623–36633